

University of Sistan  
and Baluchestan

# Chemical Process Design

Available online at <http://cpd.usb.ac.ir/>



## CFD Simulation of Drag Reduction in Horizontal Pipelines Transporting Oil-based Nano-Silica Nano-Fluids

Iman Khonsha<sup>1</sup>✉ , Kobra Salehi<sup>2</sup> , Reza Mokhtari<sup>3</sup>

<sup>1</sup>Corresponding Author, Department of Chemical Engineering, Faculty of Engineering, Shi.C., Islamic Azad University, Shiraz, Iran.  
Email: [iman.khonsha@iau.ac.ir](mailto:iman.khonsha@iau.ac.ir)

<sup>2</sup>Department of Chemical Engineering, Faculty of Engineering, Dar.C., Islamic Azad University, Darab, Iran.  
Email: [salehi.salehi@gmail.com](mailto:salehi.salehi@gmail.com)

<sup>3</sup>Department of Chemical Engineering, Faculty of Engineering, Shi.C., Islamic Azad University, Shiraz, Iran.  
Email: [mokhtati747@gmail.com](mailto:mokhtati747@gmail.com)

### ARTICLE INFO

**Article type:**  
*Research Article*

**Article history:**  
Received: 2025-06-23  
Received in revised form: 2025-11-04  
Accepted: 2025-11-06  
Available online: 2025-11-06

**Keywords:** : Oil; Horizontal pipelines;  
CFD Simulation; Drag reduction;  
Nano-fluids; Nano-silica

### ABSTRACT

This study innovatively investigates the effect of silica nanoparticles on crude oil pipeline flow drag reduction using computational fluid dynamics (CFD). Turbulent flow conditions were assumed for all simulations according to Reynolds number values. The results of the numerical simulations were validated against the experimental measurements, showing a maximum deviation of less than 8.6% in percentage drag reduction (DR%). The effect of some parameters such as fluid viscosity, flow velocity and pipe diameter (defined collectively by the Reynolds number) and pipe materials with various Nano-silica concentrations (0.25–1 wt.%), on drag reduction in the single-phase flow regime was investigated. Among the conditions investigated, optimal agreement with experimental results and highest drag reduction was recorded at 0.75 wt.% Nano-silica concentration at a Reynolds number of 13,931. Drag reduction has been found to increase with increasing concentrations of nanoparticles for fixed Reynolds numbers. For a fixed nanoparticle concentration, higher Reynolds number is also found to yield better drag reduction. These results confirm the effectiveness of the crude oil optimized using the nanoparticles in reducing the flow resistance under turbulent flow.

**Cite this article:** Khonsha, I., Salehi, K., Mokhtari, R., (2026), CFD Simulation of Drag Reduction in Horizontal Pipelines Transporting Oil-based Nano-Silica Nano-Fluids, *Chemical Process Design*, 5(1), 14-28. <http://doi.org/10.22111/cpd.2025.52433.1062>



© The Author(s).

Publisher: University of Sistan and Baluchestan.

DOI: <http://doi.org/10.22111/cpd.2025.52433.1062>

### 1. Introduction

Hydrocarbon pipeline transportation is an essential part of current energy systems since it is an excellent and relatively safe way of conveying crude oil and its products from production facilities to refineries, storage facilities, and

distribution facilities. Yet, apart from the apparent simplicity of the hydraulic process that this phenomenon may reflect, it is riddled with numerous challenges and complexities, primarily those that occur as a direct result of the pressure drop phenomenon, whose impacts on the overall efficiency, safety, and economic viability of pipeline systems can be quite substantial [1, 2]. A great portion of this pressure drop arises from frictional losses between the fluid and pipe wall. Turbulent flow conditions add to the frictional resistance encountered even more. Drag is a mechanical force that arises as an aftermath of the interaction between a solid object and a fluid medium. It is not formed by field forces such as gravitational or electromagnetic fields where the body has the potential to influence another in an absence of contact [3]. Drag reduction is an overall solution for the issue and is utilized to reduce flow resistance [4].

The technologies of pipeline drag reduction are mainly constituted of rib drag reduction, viscous drag reduction, bionic drag reduction, and vibration drag reduction of the wall, among which the drag reducer technology is a type of viscous drag reduction [5-6]. The most straightforward benefit of employing drag-reducing agents in pipeline systems is to minimize pressure drop and friction, resulting in less energy being consumed by fluid transfer pumps. The use of additive drag reduction methods can likely increase pipeline capacity, minimize associated risks, conserve capital for pipelines and pump stations, and lower operating and maintenance costs. In conclusion, the effective use of a drag reducer is cost-effective [7-8]. There are a number of techniques through which these losses can be compensated, and the addition of drag-reducing agents (DRAs) has been shown to be the most effective method [9-12].

Common drag-reducing agents include surfactants, nanoparticles, and polymeric additives. Nano-fluids are suspensions of nanoparticles (at least one dimension smaller than 100 nm) in a carrier fluid such as water, alcohol, or oil, and during the recent three decades, their greater thermal conductivity and effective heat transfer behavior have been observed by many researchers [13-17]. Depending on the nature of nanoparticles utilized, the Nano-fluids could be classified into various categories: (a) metal-based, (b) metal-oxide-based, (c) carbon-based, and (d) composite/mixed-based. Two mechanisms are suggested to facilitate drag reduction through the application of Nano-fluids in pipeline flow systems: (a) alteration of the rheological characteristics of the base fluid when nanoparticles are added, such that the delayed transition to turbulence will serve as a factor to drag reduction due to the low drag experienced with laminar flow; consequently, drag reduction for the entire pipeline is achieved [4]. (b) The decrease in the pipe roughness is a result of interactions between the nanoparticles which fill the microscopic surface asperities. This phenomenon has particular application to nanoparticles exhibiting tribological properties, which are the result of their unique morphology and exceptional strength. One appropriate example of such nanoparticles is Nano-silica, which is economical and more prevalent than other nanoparticles with comparable properties [18].

Ren et al. (2019) reported experimental verification of drag reduction in aqueous solutions with a micro-Nano composite structure. The drag reduction rate was identified to be excellent based on simulation results. The advantages that are accompanied by this phenomenon are energy saving [19]. SiO<sub>2</sub> nanoparticles were utilized as effective, non-expanding drag-reducing additives in the work of Gharekhani et al. (2021). This study took into account the influence of four various parameters on drag reduction: flow rate, nanoparticle concentration, temperature, and pipe diameter. Based on a novel methodological strategy, the experimental data (in the form of percent of drag reduction) were analyzed using an artificial neural network optimized with a genetic algorithm [3]. Shi and Jing et al. (2022) conducted a comprehensive investigation of the tribological effects of adding SiO<sub>2</sub> nanoparticles to certain

polyacrylamide (PAM) polymer solutions. Results indicated that adding SiO<sub>2</sub> nanoparticles to a cationic polyacrylamide solution resulted in the successful friction and drag reduction at Reynolds numbers greater than 6000, but at lower Reynolds numbers, nanoparticle addition had a negative impact. They discovered that the incorporation of SiO<sub>2</sub> nanoparticles into the PAM solution has a twofold effect: one is to enhance the resistance to flow as a result of the Brownian motion of the nanoparticles, while the other is to decrease the resistance to flow and shield the polymer chains from shear degradation at high shear stress levels. At the optimum nanoparticle concentration and at higher Reynolds numbers, the second phenomenon is predominant, thereby further increasing the friction-reduction effectiveness of drag-reducing polymers [20].

Ghavami Far et al. (2022) conducted numerical and experimental studies of drag reduction and heat transfer enhancement in a vertical pipe with water-polyisobutylene-Nano SiO<sub>2</sub> poly-Nano-fluids under constant heat flux conditions. The Reynolds numbers of all the prepared solutions were between 7000-22000. Nano SiO<sub>2</sub> particles with an average size of 20 nm and a concentration of 0.1-1 wt.% were dispersed in aqueous polyisobutylene solutions (base fluids) with concentrations ranging from 10-50 ppm. The optimum concentrations of nanoparticles and polymer in the prepared Nano-fluid, polymer solution, and poly-Nano-fluids were found to be 0.75wt. and 50ppm, respectively. At this optimum concentration, the Nano-fluid's coefficient of friction was noted to reduce by 75% compared to that of pure water. ANSYS fluent software package was used for validation of the experimental findings as well as simulating the phenomena associated with heat transfer and drag reduction at the established optimum conditions. The findings demonstrated an acceptable degree of concordance between the experimental and numerical data, as a deviation of less than 5% was observed [21].

With a functionalized magnetic TiO<sub>2</sub> Nano Photocatalyst and dipalmitoylphosphatidylcholine lecithin on turbulent flow drag reduction in four horizontal pipelines was investigated [22]. In a similar study, the influence of incorporating Nano-fluids made up of magnesium oxide nanoparticles and polyacrylamide polymer on decreasing the drag force in turbulent water flow in a rough horizontal pipe was investigated by Esfandiari and Hesami (2021). For the aforesaid purpose, three effective process parameters (concentration of nanoparticle, surfactant concentration, and Reynolds number) were investigated and optimized for all the pipelines. The maximum drag force reduction was 82% using numerical optimization method [23]. Here in this research work, as an innovation, simulation and optimization of drag reduction of single-phase oil flow were done by using silica nanoparticles in various concentrations and various Reynolds numbers. For this purpose, computational fluid dynamics (CFD) was used, and the numerical results were validated with and compared against experimental results.

## 2. Computational

### 2.1. CFD Modeling

The Navier–Stokes equations in ANSYS Fluent are solved in conservative form in cylindrical coordinates, represented by the continuity and momentum equations [24]. The continuity equation for incompressible fluids with constant density is expressed as [24]:

$$\text{grad}(\rho v) = 0 \quad (1)$$

The momentum equation is [24]:

$$\rho \left( \frac{\partial V}{\partial t} + V \cdot \text{grad}(V) \right) + \text{grad}(p) - \text{div}(2\eta(\dot{\gamma})\dot{\gamma}) = 0 \quad (2)$$

In this equation,  $V$  represents the velocity,  $\rho$  denotes the fluid density,  $p$  signifies the pressure, and  $\dot{\gamma}$  is the stress tensor rate, which is derived from Eq. (3) [24].

$$\dot{\gamma} = (1/2) [gradV + (gradV)^T] \quad (3)$$

For Newtonian fluids, the viscosity is constant and independent of the shear rate, expressed by  $\eta(|\dot{\gamma}|) = \mu$ . Conversely, for dilute non-Newtonian fluids, the Power Law model is commonly used to describe the shear-dependent viscosity, i.e., viscosity  $\eta(|\dot{\gamma}|) = k|\dot{\gamma}|^{(n-1)}$ , where  $k$  is the consistency index and  $n$  is the flow behavior index [24]. Furthermore, the introduction of nanoparticles in the base fluid tends to increase the viscosity [18, 25, 26].

For turbulent flows, the effects of velocity and pressure fluctuations must be incorporated into the governing equations. One common approach is the Reynolds-Averaged Navier–Stokes (RANS) formulation, in which instantaneous flow variables are decomposed into mean and fluctuating components, as shown in Eq. (4). The averaging procedure yields the RANS equations, which describe the mean flow behavior but also introduce additional terms, known as Reynolds stresses that account for the effects of turbulence [27].

$$\rho \left( \frac{\partial \bar{V}}{\partial t} + \bar{V} \cdot \nabla \bar{V} \right) = -grad(\bar{p}) + \mu \nabla^2 \bar{V} - \rho \nabla \cdot \bar{V}'\bar{V}' \quad (4)$$

where  $\bar{V}$  and  $\bar{p}$  denote the mean velocity and pressure, respectively, while  $\bar{V}'\bar{V}'$  represents the Reynolds stresses. The standard k- $\epsilon$  turbulence model was employed due to its proven numerical stability, computational economy, and suitability for internal flows such as pipe flow. This model has been widely applied in studies of non-Newtonian nanofluid flows and has been shown to be in good agreement with experimental data. Furthermore, the accompanying wall function method allows for accurate and efficient computation of near-wall turbulence effects without requiring excessive mesh refinement [28].

## 2.2. Geometry and Mesh

Five pipes, which were 9 meters long and had varying diameters as indicated in Table 1 and Fig. 1, were being considered for use in the study. The first pipe was characterized by a smooth and highly polished inner surface, while the other pipes had a similar surface roughness.

As shown in Fig. 2, a uniform hexahedral mesh was employed for the computational domain of the cylindrical pipe to ensure good spatial accuracy and numerical stability. Local mesh refinement was utilized near the walls to accurately capture steep velocity gradients and capture the formation of the boundary layer, which is crucial in simulating the non-Newtonian character of nanoparticle-enhanced crude oil. The cross-section at the inlet was discretized uniformly to facilitate stable initialization of the flow field.

**Table 1.** Specifications of the pipes used in this study [18]

Pipe No.	Pipe diameter (m)	Material	Roughness (m)
1	0.0127	5-layer unique	0.000046
2	0.0127	Galvanized iron	0.000152
3	0.01905	Galvanized iron	0.000152
4	0.0254	Galvanized iron	0.000152
5	0.03175	Galvanized iron	0.000152

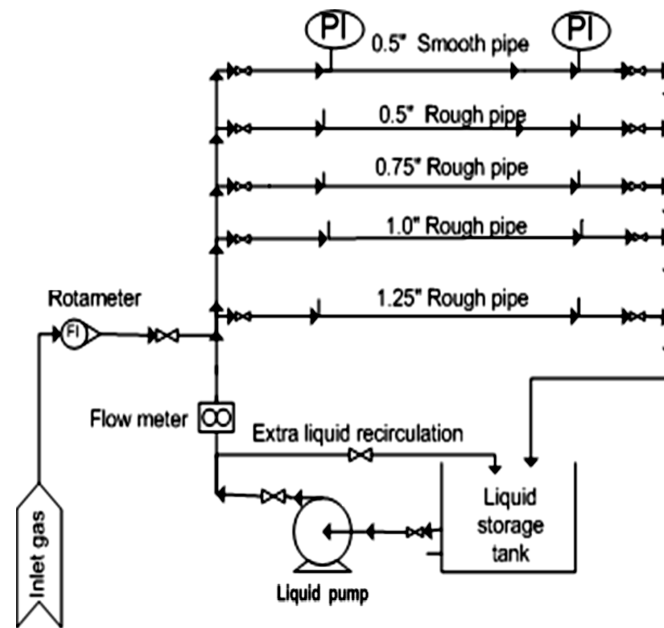


Fig. 1. Schematic of the pipes under investigation with different surface roughness [18]

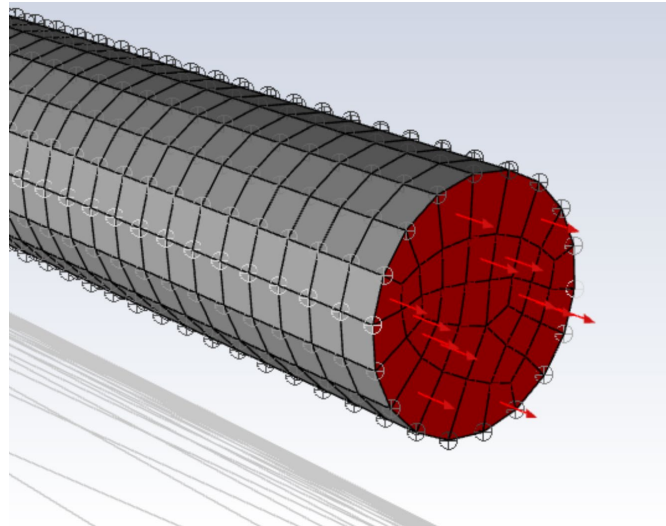
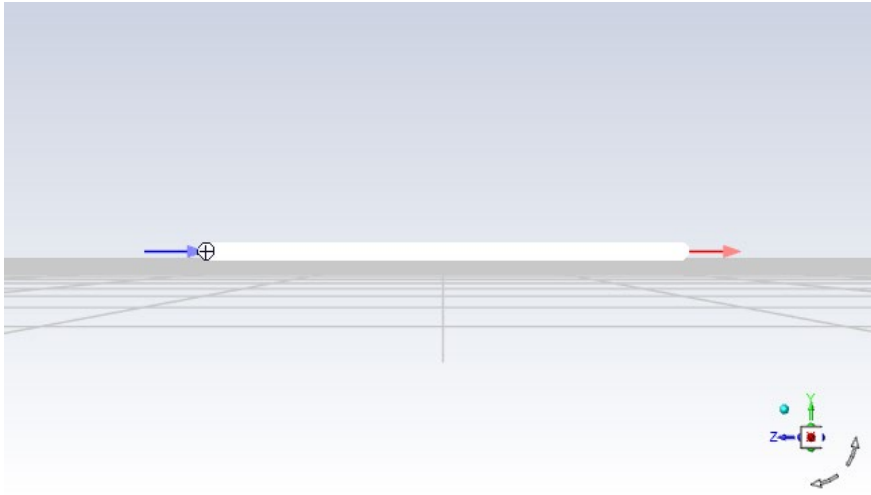


Fig. 2. A view of the pipe geometry and meshing in ANSYS Fluent software

Fig. 3 shows the geometry and boundary conditions of the pipe. Since the pipe flow was assumed to be steady and continuous, a constant velocity boundary condition was applied at the inlet and a constant pressure (outflow) condition was applied at the outlet. No-slip wall boundary conditions were applied to simulate the pipe walls, and axial symmetry was applied along the central axis to simulate the symmetry of the cylindrical geometry [29].

Single-phase fluid flow was investigated in the first phase of the research. A single inlet and a single outlet were allocated to each conduit, and the side walls were regarded as solid boundary walls. Individual reservoir crude oil was supplied into each pipe, and the corresponding pressure drop was measured at various Reynolds numbers. In the second phase, a specified concentration of Nano-silica was introduced into the oil reservoir. Once a steady-state was reached, pressure drop measurements were renewed with the same flow conditions. The percentage drag reduction (DR%) was calculated as the ratio of the difference in the frictional pressure drop when nanoparticles were introduced to that of the base fluid under identical operating conditions.



**Fig. 3.** the geometry and boundary conditions of the pipe

$$DR\% = \frac{|\Delta p_f - \Delta p_{f, DRA}|}{\Delta p_f} \times 100 \quad (5)$$

Assumptions in the simulation were: the geometry was assumed to be three-dimensional, and the hydrodynamic condition was taken for steady state. Crude oil was selected as the base fluid in the Materials panel of ANSYS Fluent. The default Newtonian viscosity model (constant viscosity) was replaced with a non-Newtonian Power Law model to simulate the shear-dependent rheological response of the nanoparticle-enhanced crude oil more accurately. The consistency index ( $k$ ) and flow behavior index ( $n$ ) were taken from experimental results reported in reference [18]. Additionally, the effective viscosity at different volume fractions of nanoparticles was approximated through Einstein's equation incorporated within the Power Law model for simulating the variation of viscosity with nanoparticle concentration more realistically.

Owing to the low volume fraction of nanoparticles, Einstein's relation ( $\mu_{\text{Nano-fluid}} = \mu(1 + 2.5\phi_s)$ )—where  $\phi_s$  is the solid particle volume fraction and  $\mu$  is the viscosity of the solvent in the absence of solid particles—is employed to calculate the viscosities of the solutions as a direct function of the mass fraction of materials concerned. All the parameters have been set at exactly  $10^{-5}$  [30] as the convergence criterion. Simulations were carried out at a constant temperature. QUICK scheme was employed in the discretization of all the terms owing to its very high accuracy, whereas the SIMPLE algorithm was utilized in the management of velocity and pressure variables owing to their quicker solution process and very low computational cost. The system of computations employed was 64-bit with a RAM of 16 GB and an 8-core processor operating at a clock rate of 3.2 GHz. Moreover, because the fluid flow within the piping system was considered to be continuous in nature, a constant velocity inlet and constant pressure outlet have been chosen as boundaries. Walls of the pipes are modeled using a wall boundary condition along with a no-slip condition. Physical characteristics of the silica nanoparticles and crude oil used here have been taken from Pouranfard et al. as mentioned in Table 2 [18].

**Table 2.** Silica nanoparticle specifications [18] and Crude oil density and rheological parameters

Silica specifications	Morphology	Diameter (nm)	Specific Surface area (m <sup>2</sup> /g)	Actual density (g/cm <sup>3</sup> )
	Approximately spherical	20-30	180-600	2.4
Crude oil density and rheological parameters	Density (kg/m <sup>3</sup> )	Temperature (°C)	Fluid consistency Index (kg/(m·s <sup>(2-n)</sup> ))	Flow behavior index (-)
	830	25	0.009	0.71

In Table 2,  $n$  and  $k$  are two key parameters of the fluid consistency index and the flow behavior index, which are used in Eq. (6) for non-Newtonian fluids.

$$\tau_w = k \left( \frac{du}{dy} \right)^n \quad (6)$$

In this study, no experimental investigation was conducted and experimental data from reference [18] were used to validate the simulation results.

### 3. Results and discussion

#### 3.1. Investigating the independence of results from network size

Numerical solution of the model was carried out using computational fluid dynamics (CFD) software ANSYS Fluent version 2020. The software was used due to its complete and diverse methods, its high capability in designing various geometries, and its elimination of the need for other meshing software. To achieve the most appropriate mesh size, pipe number 1 with the dimensions given in Table 1 was used with an inlet Reynolds number of 10,449 and a 1% weight mixture of silica nanoparticles in oil. Fig. 4 is the velocity profile plotted against the dimensionless diameter ( $r/R$ ), in a cross-section 2 meters downstream from the inlet, where  $R$  is the pipe diameter and  $r$  is the system diameter. The two-dimensional mesh grid had 98,765, 187,432, 207,626, and 278,932 elements, respectively. These mesh options are a mix of structured and unstructured meshes, which are very appropriate for complex geometries.

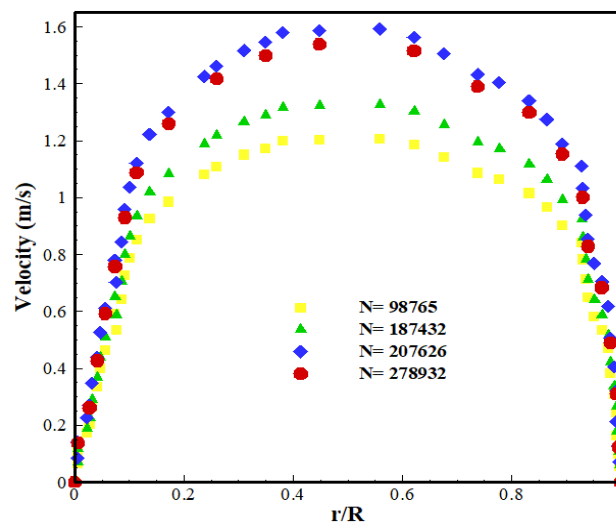


Fig. 4. System meshing at different scales

In the above diagram, the velocity at the walls is zero due to the no-slip condition, and the maximum velocity in the center of the pipe is observed at 1.6 m/s. According to this figure, when the number of mesh elements increases from 207,626 to 278,932, there is a reduction in the fluctuations of velocity along the radius of the pipe at the outlet section, with a difference of 12.5% between the two cases. Therefore, in order to save computational expense, 207,626 elements were utilized.

#### 3.2. Model validation

Model validation was achieved by a comparison between the results of the simulation and the system's actual outputs. To this end, the experimental data of Pouranfard et al. [18] for pipe number 1 with Reynolds number 6966, was

utilized. The validation results are presented in Fig. 5, where the horizontal axis is the weight percentage of silica nanoparticles, and the vertical axis is the percentage of drag reduction.

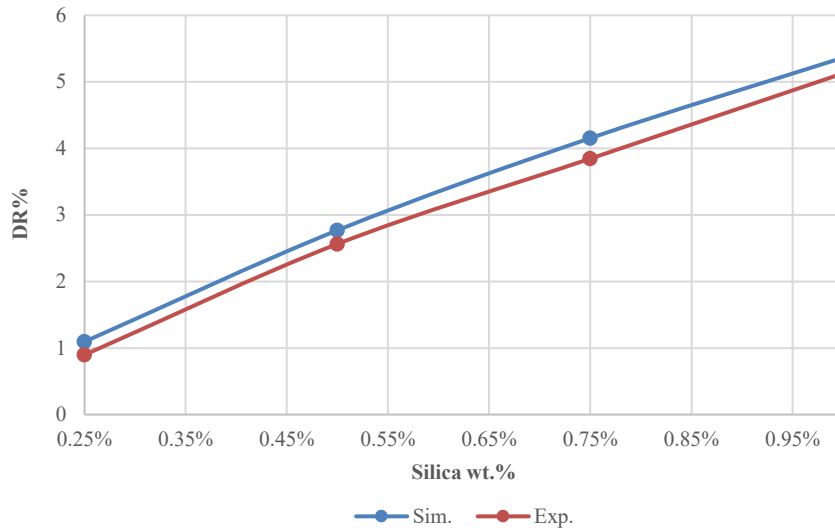


**Fig. 5.** Validation of simulation results using experimental data at a constant Reynolds number of 6966

As indicated in Fig. 5, the overall difference between the simulation result and experimental data is approximately 12%. The difference can be due to the type of mesh or boundary condition implemented. However, the coincidence of the results shows that the model implemented is adequate to model the process.

### 3.3. Effect of Reynolds number and Nano-silica concentration on drag reduction

The percentage reduction in the drag of the oil/Nano-silica flow as a function of Nano-silica concentration for different Reynolds numbers in pipes 1- 5 are shown in Figs. 6-10 respectively.

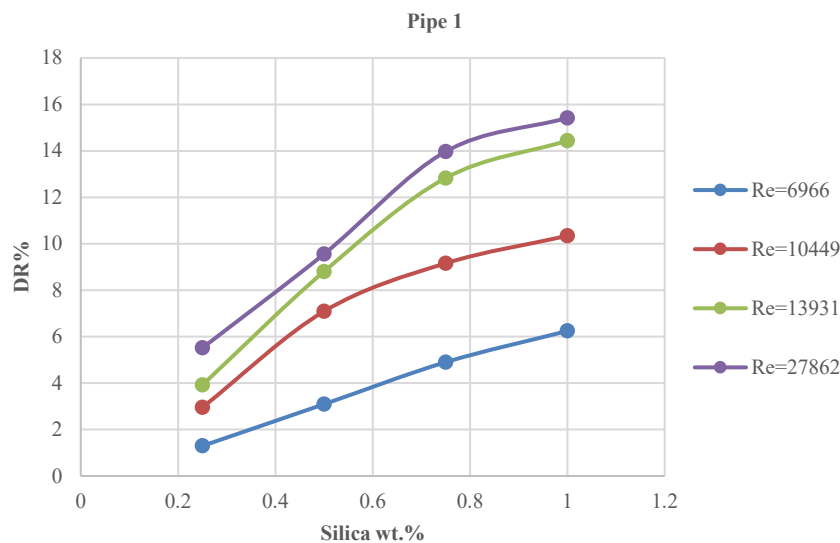


**Fig. 6.** Drag reduction percentage of the oil/Nano-silica flow as a function of Nano-silica concentration in pipe number 1 at different Reynolds numbers

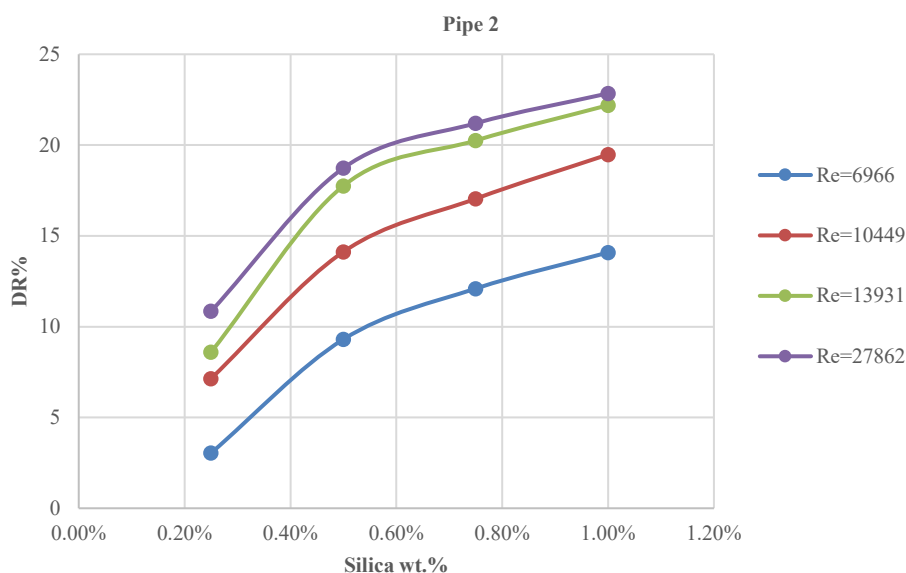


**Fig. 7.** Drag reduction percentage of the oil/Nano-silica flow as a function of Nano-silica concentration in pipe number 2 at different Reynolds numbers

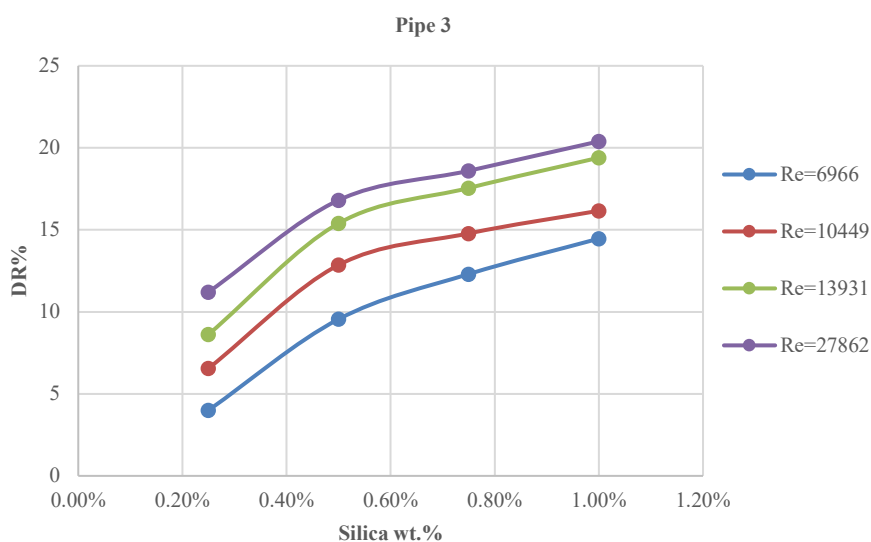


**Fig. 8.** Drag reduction percentage of the oil/Nano-silica flow as a function of Nano-silica concentration in pipe number 3 at different Reynolds numbers

As evident from these results, the increase in silica nanoparticles reduces drag and hence pressure drop. These results are consistent with the findings of Esfandiari et al. [23], where addition of silica nanoparticles also led to higher drag reduction at high Reynolds numbers due to the suppression of the turbulence mechanism.

Further, at a constant Reynolds number, a rise in the concentration of silica nanoparticles enhances the percentage drag reduction. With a constant mechanical energy expenditure, the increase in the Reynolds number increases the percentage of drag reduction. The optimal conditions in all the tubes were 0.75 wt.% silica nanoparticles and a Reynolds number of 13931, with the highest drag reduction occurring in tube number 2. Adding silica nanoparticles to oil flows results in dramatic drag reduction primarily due to modification of the rheological properties of the fluid. Silica nanoparticles alter the flow characteristic and base fluid viscosity, causing it to exhibit Newtonian tendencies. The transformation reduces the frictional forces being acted upon when the fluid flows through channels or pipes.

For instance, research showed that incorporation of a mixture of silica and magnesium oxide nanoparticles reduced the viscosity of crude oil to a large degree, with maximum percentage viscosity reduction of 56.91% at high temperatures and concentrations, consequently leading to maximum drag reduction up to 53.17% [31].

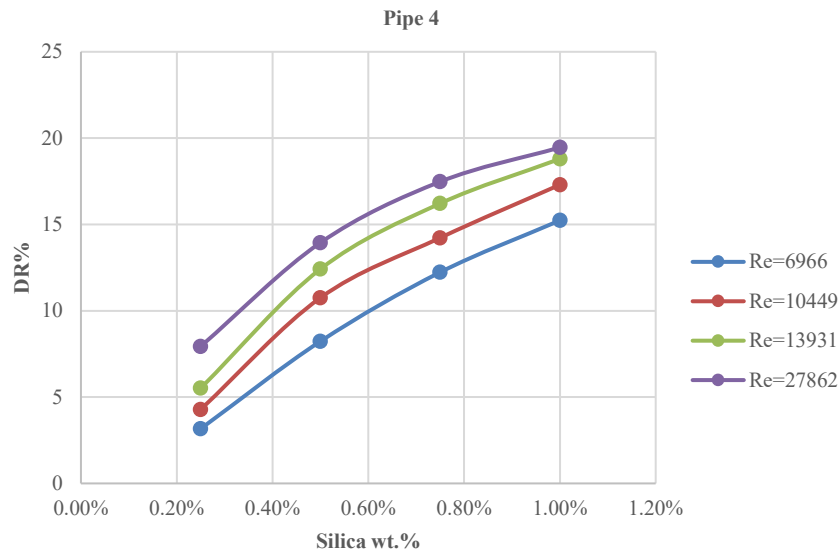


**Fig. 9.** Drag reduction percentage of the oil/Nano-silica flow as a function of Nano-silica concentration in pipe number 4 at different Reynolds numbers

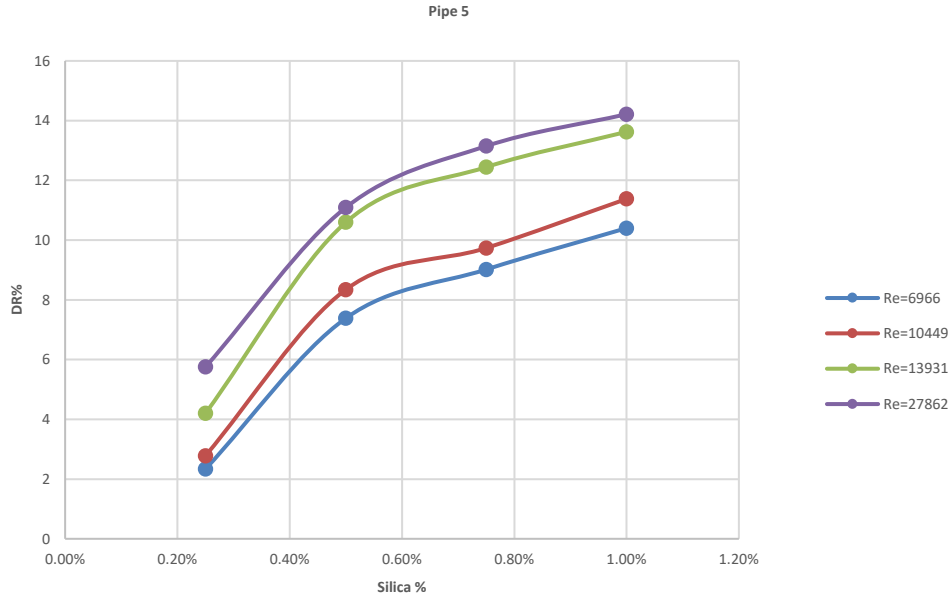


**Fig. 10.** Drag reduction percentage of the oil/Nano-silica flow as a function of Nano-silica concentration in pipe number 5 at different Reynolds numbers

The drag reduction effect increases with higher concentrations of silica nanoparticles due to several reasons. As concentration increases, more nanoparticles are available to interact with the oil molecules and this enhances overall modification of rheological properties of the fluid. This will decrease viscosity as well as friction factor further to a larger degree and therefore improve flow characteristics [3, 31, 32]. The second mechanism of drag reduction is nanoparticles' ability to delay onset of turbulence in the flow. By modifying the flow structure, nanoparticles can

enhance the stability of laminar regimes of flow, which tend to have lower drag than turbulent flows [3]. Silica nanoparticles in this work act as micro-scale flow modifiers [18, 25, 26], enhancing local effective viscosity, engaging with and inhibiting near-wall turbulent structures, and fragmenting the energy cascade in the turbulent boundary layer. With a rise in the Reynolds number, the turbulence becomes more matured, allowing nanoparticles to play a greater role in influencing the flow structure, thereby reducing wall shear stress and lowering pressure drop. The performance that justifies that silica nanoparticles alone can be effective drag-reducing agents in high-Reynolds-number crude oil pipeline flow systems [33].

Given the large number of simulations performed, the pressure contours in each of the five pipes under optimal conditions (Reynolds number 13931 with a concentration of 0.75%) are presented in the figures 11-15.

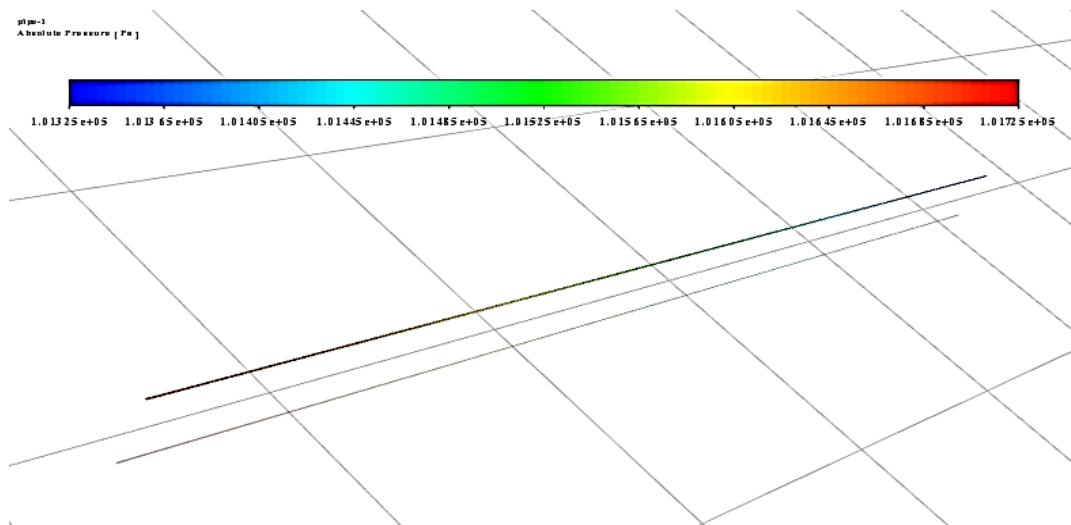


**Fig. 11.** Pressure contour of oil/Nano-silica flow in pipe number 1 at a Reynolds number of 13931 with a concentration of 0.75%

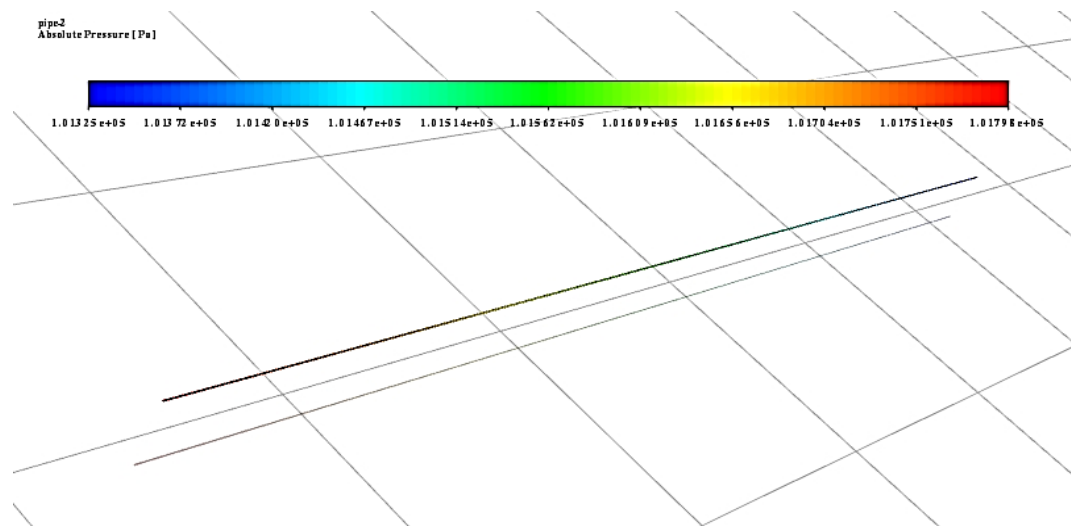


**Fig. 12.** Pressure contour of oil/Nano-silica flow in pipe number 2 at a Reynolds number of 13931 with a concentration of 0.75%

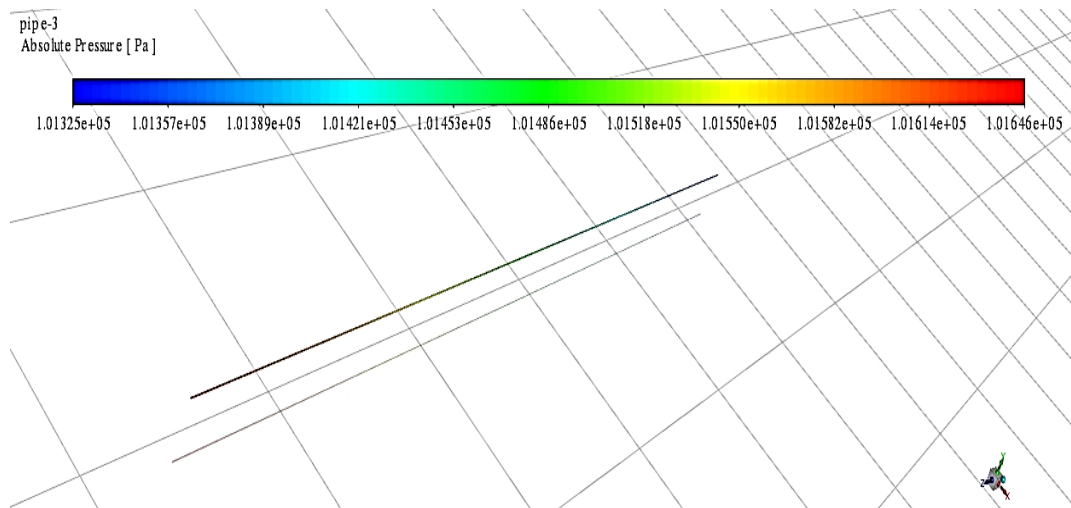


**Fig. 13.** Pressure contour of oil/Nano-silica flow in pipe number 3 at a Reynolds number of 13931 with a concentration of 0.75%

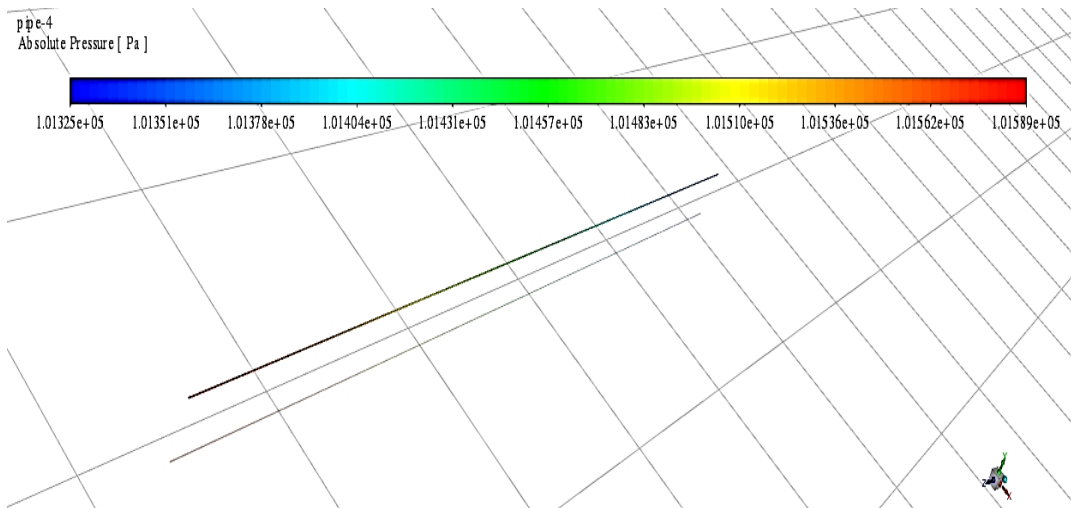


**Fig. 14.** Pressure contour of oil/Nano-silica flow in pipe number 4 at a Reynolds number of 13931 with a concentration of 0.75%

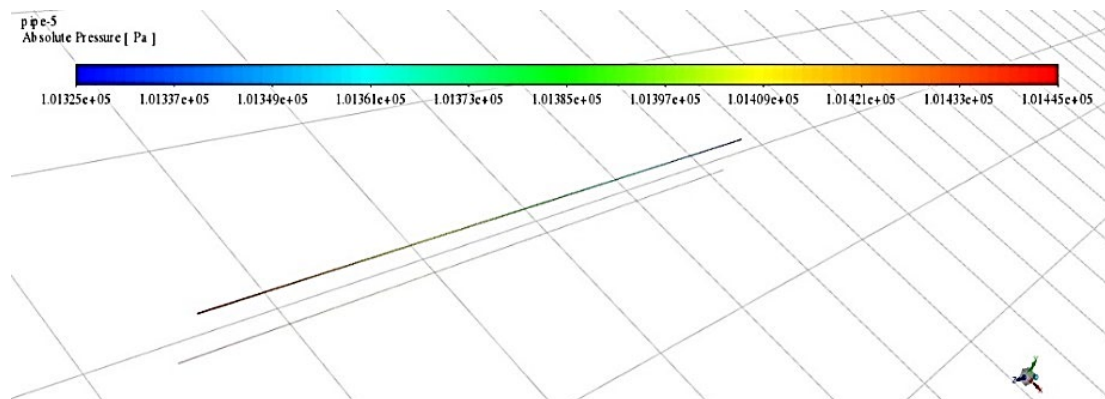


**Fig. 15.** Pressure contour of oil/Nano-silica flow in pipe number 3 at a Reynolds number of 13931 with a concentration of 0.75%

In these images, warm colors (red, orange) symbolize regions of higher pressure, and cool colors (blue, green) symbolize regions of lower pressure. The transition from warm to cool colors along the pipe shows the pressure drop along the direction of flow. In addition, more compact contour lines (with less distance between them) symbolize a greater-pressure gradient, and lines with more spacing symbolize homogeneity or a lesser pressure change. In all photos, there is a decrease in the pressure gradient in the presence of Nano-silica. This alteration symbolizes the

reduction in drag and enhanced energy transfer. Pipe number 1 demonstrates a pressure distribution showing a gradual and proportional pressure reduction along the pipe. In the vicinity of the walls, the pressure reduction is less, which signifies the reduction in drag by the presence of Nano-silica. In pipe number 2, the existence of an irregular pressure gradient in certain regions signifies the possibility of local turbulence. Geometric fluctuations or pipe roughness can produce vortex areas. In pipe number 3, the pressure is more evenly distributed, which implies that the utilization of Nano-silica has lowered turbulence and enhanced pressure homogeneity. The pattern of contours in pipe numbers 4 and 5 seems comparable to those seen in the preceding pipes, but it might have a gradual pressure reduction with more localized fluctuations. This might be the outcome of slight geometrical changes or flow effects.

Figure 16 concerning the gradient in the pipe cross-section. As observed in the figure, velocity is maximum at the center of the pipeline and reduces progressively to zero as it moves towards the pipe wall owing to friction between the pipe and the fluid.

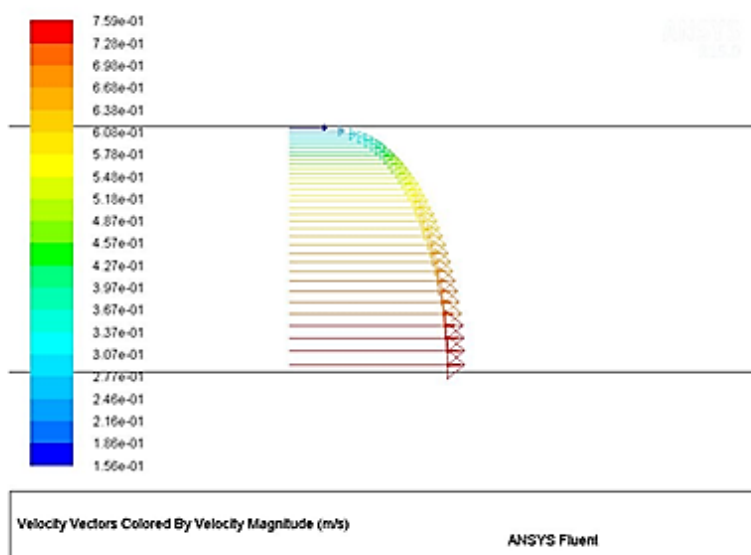


Fig. 16. The gradient in the cross-section of the pipe due to the addition of Nano-silica

#### 4. Conclusion

This work investigated the application of silica nanoparticle-based crude oil Nano-fluids as new drag-reducing agents in pipeline transportation systems. Through computational fluid dynamics (CFD) simulations in ANSYS Fluent, the effects of different operating parameters—especially fluid viscosity, flow velocity and pipe diameter (defined collectively by the Reynolds number) and surface roughness—on the drag reduction behavior were investigated systematically. The numerical simulation indicated that the addition of silica nanoparticles caused drag reduction particularly at high Reynolds numbers because of the suppression of the turbulence. Moreover, the increase in silica nanoparticle concentration in the crude oil always caused greater drag reduction for all the Reynolds numbers investigated. Specifically, the simulation demonstrated a clear positive correlation between nanoparticle concentration and drag reduction capability under constant flow conditions. At constant nanoparticle concentration, however, the percentage drag reduction increased as Reynolds numbers increased, indicating the growing contribution of turbulence effects in facilitating nanoparticle-induced flow changes. Further, the research demonstrated that pipe diameter has an important influence on drag reduction results. Larger diameters of pipes manifested smaller drag reduction efficiency, which is due to changed flow dynamics and wall interaction behavior.

This finding is especially important for the design or retrofit of pipeline systems since it indicates that pipe size optimization can be a key factor in the improvement of the performance of Nano fluid-based drag reduction approaches. The results of the simulation were compared with experimental data, in which there was good conformity with a maximum deviation of less than 8.6%, thus ensuring the reliability of the suggested CFD model. The best performance among the tested conditions occurred at a Nano-silica concentration of 0.75 wt.% and a Reynolds number of 13,931, with the highest drag reduction in the second pipe configuration. In summary, this study gives insightful information about the feasibility of using silica-based Nano fluids as a drag reducer in crude oil transport. The results set the stage for experimental and field-scale studies, providing a promising avenue for energy conservation and flow optimization in petroleum pipeline transportation.

## Nomenclature

Symbols		Greek symbols	
k	Consistency index	$\dot{\gamma}$	Stress tensor rate
n	Flow behavior index	$\mu$	Viscosity
p	Pressure	$\rho$	Density
R	Pipe diameter	$\phi_s$	Solid particle volume fraction
r	System diameter	$\tau_w$	Wall shear stress
t	Time	$\rho$	Density
V	Velocity	Abbreviation	
$\bar{V}$	Mean velocity	CFD	Computational Fluid Dynamics
$\overline{V'V'}$	Reynolds stresses	DRA	Drag Reducing Agent
$\Delta p_f$	Frictional pressure drop before adding DRA	DR%	Drag Reduction Percentage
$\Delta p_{fDRA}$	Frictional pressure drop after adding DRA	RANS	Reynolds-Averaged Navier–Stokes
		Re	Reynolds Number

## Conflict of interest statement

There is no actual or potential conflict of interest concerning this article.

## References

- [1] Hart, A., 2014. A review of technologies for transporting heavy crude oil and bitumen via pipelines, *Journal of Petroleum Exploration and Production Technology*, 4, 327. <https://doi.org/10.1007/s13202-013-0086-6>
- [2] Wei, L., Zhang, y., Ji, L., Ye, L., Zhu, X., Fu, J., 2022. Pressure drop prediction of crude oil pipeline based on PSO-BP neural network, *Energies* 15, no. 16: 5880. <https://doi.org/10.3390/en15165880>
- [3] Gharekhani, F., Ardjmand, M., Vaziri, A., 2021. Experimental study of drag reduction phenomena in the horizontal tube with nano SiO<sub>2</sub> by neural network-genetic algorithm, *Iranian Journal of Chemistry and Chemical Engineering*, 40,1304. <https://doi.org/10.30492/ijcce.2021.131778.4256>
- [4] Pouranfard, A., Mowla, D., Esmailzadeh, F., 2014. An experimental study of drag reduction by nanofluids through horizontal pipe turbulent flow of a Newtonian liquid, *Journal of Industrial and Engineering Chemistry* 20, 633–637. <https://doi.org/10.1016/j.jiec.2013.05.026>
- [5] Sohn, J.I., Kim, C.A., Choi, H.J., Jhon, M.S., 2001. Drag-reduction effectiveness of Xanthan gum in a rotating disk apparatus. *Carbohydrate Polymers*, 45. 61-68. [https://doi.org/10.1016/S0144-8617\(00\)00232-0](https://doi.org/10.1016/S0144-8617(00)00232-0)
- [6] Gómez Cuenca, F., Gómez Marín, M. and Folgueras Díaz, M.B., 2008. Energy-savings modeling of oil pipelines that use drag-reducing additives, *Energy and fuels*, 22(5), 3293-3298. <https://doi.org/10.1021/ef800364a>
- [7] Amorim, B.H.S., Pires, L., Menezes, I., Montalvão, A.F.F., 2018. Proceedings of the 2018 12th International Pipeline Conference. 24-28 (Calgary, Alberta, Canada). <https://doi.org/10.1115/IPC2018-78619>
- [8] Al-Sarkhi, A.,2013. Effects of drag-reducing polymers on stratified and slug gas–liquid flows in a horizontal pipe, *Arabian Journal for Science and Engineering*, 38, 699. <https://doi.org/10.1007/s13369-012-0520-y>
- [9] Cheng, Z., Zhang, X., Song, X., Wang, X., Zhang, G., Lu, Y., Li, L., Liu, F., Dai, X., 2023 Investigation of Drag Reduction by Slurry-Like Drag-Reducing Agent in Microtube Flow Using Response Surface Methodology (RSM). *Scientific Report*, 13, 22433. <https://doi.org/10.1038/s41598-023-49804-9>
- [10] Cheng, Z., Zhang, X., Dai, X., Zhai, H., Song, X., Wang, X., Gao, L., Zhang, G., Lu, Y., Li, L., Yan, X., Zhang, J., 2024. Experimental Study on the Drag Reduction Performance of Sodium Alginate in Saline Solutions, *Scientific Report*, 14, 32123. <https://doi.org/10.1038/s41598-024-83910-6>
- [11] Sreedhar, i., Sai Darshan, A., Srivastava, A., Jain, V., 2018. Complex Behavior of Polymers as Drag Reducing Agents Through Pipe Fittings, *Journal of Applied Fluid Mechanics*, 11(2), 467-474. <https://doi.org/10.1007/s13399-021-02077-6>

- [12] AL-Dogail, A., Gajbhiye, R., Patil, S., 2023. A review of drag-reducing agents (DRAs) in petroleum industry, *Arabian Journal for Science and Engineering* 48, 8287. <https://doi.org/10.1007/s13369-022-07184-8>
- [13] Chakraborty, S., Sarkar, I., Ashok, A., Sengupta, I., 2018. Synthesis of Cu-Al LDH nanofluid and its application in spray cooling heat transfer of a hot steel plate, *Powder Technology*, 335, 285. <https://doi.org/10.1016/j.powtec.2018.05.004>
- [14] Wusiman K., Jeong, H., Tulugan, K., Afrianto, H., 2013. Thermal performance of multi-walled carbon nanotubes (MWCNTs) in aqueous suspensions with surfactants SDBS and SDS. *International Communications in Heat and Mass Transfer*, 41, 28. <https://doi.org/10.1016/j.icheatmasstransfer.2012.12.002>
- [15] Indhuja, A., Suganthi, K. S., Manikandan, S., Rajan, K.S., 2013. Viscosity and thermal conductivity of dispersions of gum arabic capped MWCNT in water: Influence of MWCNT concentration and temperature, *Journal of the Taiwan Institute of Chemical Engineers*, 44, 474. <https://doi.org/10.1016/j.jtice.2012.11.015>
- [16] Yu, W., Xie, H., Chen, L., Li, Y., 2010. Enhancement of thermal conductivity of kerosene-based Fe<sub>3</sub>O<sub>4</sub> nanofluids prepared via phase-transfer method, *Colloids and Surfaces A Physicochemical and Engineering Aspects*, 355, 109. <https://doi.org/10.1016/j.colsurfa.2009.11.044>
- [17] Li, D., Hong, B., Fang, W., Guo, W. Lin, R., 2010. Preparation of well-dispersed silver nanoparticles for oil-based nanofluids, *Industrial and Engineering Chemistry Research*, 49, 1697. <https://doi.org/10.1021/ie901173h>
- [18] Pouranfard, A., Mowla, D. Esmailzadeh, F., 2015. An experimental study of drag reduction by nanofluids in slug two phase flow of air and water through horizontal pipes, *Chinese Journal of Chemical Engineering* 23(3), 471. <https://doi.org/10.1016/j.cjche.2014.11.023>
- [19] Ren, X., Yang, L., Li, C., Cheng, G. Liu, N., 2019. Design and analysis of underwater drag reduction property of biomimetic surface with micro-nano composite structure, *Journal of Mechanisms and Machine Science*, 546-559. [https://doi.org/10.1007/978-981-32-9941-2\\_45](https://doi.org/10.1007/978-981-32-9941-2_45)
- [20] Li, X., Pan, J., Shi, J., Chai, Y., Hu, S., Han, Q., Zhang, Y., Li, X., Jing, D., 2022. Nanoparticle-induced drag reduction for polyacrylamide in turbulent flow with high Reynolds numbers. *Chinese Journal of Chemical Engineering*. 56, 290. <https://doi.org/10.1016/j.cjche.2022.07.015>
- [21] Ghavamifar, S., Pouranfard, A. Shamsi, M., 2024. Experimental and numerical study of drag reduction and heat transfer enhancement in a vertical pipe using water/polyisobutylene/nano-SiO<sub>2</sub> polynanofluids, *Journal of Dispersion Science and Technology* 45, 1. <https://doi.org/10.1080/01932691.2023.2165093>
- [22] Esfandiari, N., Zareinezhad, R., Habibi, Z., 2020. The investigation and optimization of drag reduction in turbulent flow of Newtonian fluid passing through horizontal pipelines using functionalized magnetic nanophotocatalysts and lecithin, *Chinese Journal of Chemical Engineering*, 28, (1), 63-75. <https://doi.org/10.1016/j.cjche.2019.04.015>
- [23] Hesami, M., Esfandiari, N., 2021. Experimental Investigation of Drag Reduction in a Rough Horizontal Pipeline Using Nanofluid by Surface Response Method, *Nashrieh Shimi va Mohandesi Shimi Iran*, 40(2) 2, 239-246.
- [24] Devals, C., Heniche, M., Takenaka, K., Tanguy, P.A., 2008. CFD analysis of several design parameters affecting the performance of the maxblend impeller. *Computers and Chemical Engineering*, 32, 1831. <https://doi.org/10.1016/j.compchemeng.2007.09.007>
- [25] Raei, B., Shahraki, F., Jamialahmadi, M., & Peyghambarzadeh, S. M., 2016. Experimental investigation on the heat transfer performance and pressure drop characteristics of  $\gamma$ -Al<sub>2</sub>O<sub>3</sub>/water nanofluid in a double tube counter flow heat exchanger. *Challenges in Nano and Micro Scale Science and Technology*, 5(1), 64-75. <https://doi.org/10.7508/tpnms.2017.01.007>
- [26] Masuda, H., Ebata, A., Teramae, K. and Hishinuma, N., 1993. Alteration of Thermal Conductivity and Viscosity of Liquid by Dispersing Ultra-Fine Particles. Dispersion of Al<sub>2</sub>O<sub>3</sub>, SiO<sub>2</sub> and TiO<sub>2</sub> Ultra-Fine Particles. *Netsu Bussei*, 7, 227-233. <https://doi.org/10.2963/jjtp.7.227>
- [27] Li, Z., Hu, H., Du, P., Xie, L., Wen, J., & Chen, X., 2023. Reynolds-averaged simulation of drag reduction in viscoelastic pipe flow with a fixed mass flow rate. *Journal of Marine Science and Engineering*, 11(4), 685. <https://doi.org/10.3390/jmse11040685>
- [28] Begag, A., Saim, R., Öztop, H. F., & Abboudi, S. (2021). Numerical Study on Heat Transfer and Pressure Drop in a Mini-Channel with Corrugated Walls, *Journal of Applied and Computational Mechanics*, 7(3), 1306-1314. <https://doi.org/10.22055/JACM.2020.34487.2418>
- [29] Ansys Fluent21 user's guide 2021 ANSYS FLUENT Inc,
- [30] Ayeni, O., Tiwari, S. S., Wu, C., Joshi, J. B., Nandakumar, K., 2020. Behavior of particles in a low and moderate Reynolds numbers using computational fluid dynamics-Discrete element model. *Physics of Fluids* 32 (7). <https://doi.org/10.1063/5.0008518>
- [31] Alhamd, S. J., Manteghian, M., Dehaghani, A.H.S., Rashid, F.L., 2024. An experimental investigation and flow-system simulation about the influencing of Silica-Magnesium oxide nano-mixture on enhancing the rheological properties of Iraqi crude oil, *Scientific Reports*, 14, 6148. <https://doi.org/10.1038/s41598-024-56722-x>
- [32] Ghamartale, A., Saboori, R., & Sabbaghi, S., 2024. The effect of micro/nano-particles on pressure drop in Oil pipeline: Simulation, *International Journal of Nano Dimension*, 7(3). <https://doi.org/10.7508/ijnd.2016.03.005>
- [33] Akindoyo, E. Abdulbari, H.A., 2015. Drag reduction efficacy of CTABr and nanosilica particles using rotating disk apparatus (RDA), *Australian Journal of Basic and Applied Science*, 9, 136.